JOURNAL OF RESEARCH of the National Bureau of Standards—C. Engineering and Instrumentation
Vol. 70C, No. 2, April–June 1966

Ellipsoidal Mirror Reflectometer*

S. Thomas Dunn [1] and Joseph C. Richmond

Institute for Basic Standards, National Bureau of Standards, Washington, D.C.

and

John A. Wiebelt

Oklahoma State University

(January 6, 1966)

A new ellipsoidal mirror reflectometer is described, in which radiant flux from an infrared monochromator is focused on a specimen placed at the first focal point of the ellipsoid and a thermopile detector is placed at the second. Errors associated with angular and areal variations in sensitivity of the detector and with aberrations in the optics were largely eliminated through use of a small averaging sphere placed over the detector. Losses caused by the presence of the entrance hole in the ellipsoidal mirror and from mirror absorption were evaluated both theoretically and experimentally. Corrections for these losses permitted absolute reflectance to be obtained for both diffuse and partially diffuse reflecting specimens. In addition, the unique optics of the ellipsoidal mirror provide more versatility than is available in previous reflectometers. This versatility includes the ability to accurately measure directional-hemispherical, specular, nonspecular, and directional-annular cone reflectance. An analysis of the accuracy of the instrument indicates that an accuracy of better than one percent is possible for all engineering materials. The use of the sulfur averaging sphere also allowed the construction of a simple accurate specular reflectometer for calibration of the mirror reference standards used in these measurements.

Key Words: Averaging spheres, bidirectional reflectance, diffuse reflectance, ellipsoidal reflectometer, infrared, infrared detectors, reflectance, reflectometer, spatial sensitivity, spectral reflectance, specular reflectance.

1. Introduction

This paper describes the development and analysis of an ellipsoidal mirror reflectometer, which has proved to be highly versatile and capable of providing reflectance data of high accuracy. Although the instrument was developed specifically for the infrared portion of the spectrum, it is equally applicable to the visible and near infrared portions.

2. Definition of Terms

The terminology used in this paper is that used in the field of radiant heat transfer. Because some of the terms have different meanings than are normally used in the field of optics, they will be defined here.

Reflectance is the fraction of incident flux that is reflected by a specimen. It will vary with the wavelength of incident flux and with the direction of propagation, relative to the surface, of the incident and reflected flux. It is thus necessary to modify the term reflectance to indicate the geometric and wavelength conditions of measurement.

Spectral, in a narrow wavelength bond centered at a specified wavelength. Spectral reflectance may be plotted as a function of wavelength to produce a *spectral reflectance curve.*

Directional, in a small solid angle about a given direction.

Hemispherical, in all possible directions from a surface.

Diffuse, incident on a surface or reflected from a surface with equal radiance in all possible directions.

Directional hemispherical reflectance is the fraction of the flux incident in a small solid angle $\Delta\omega$ about the direction φ, θ, that is reflected into the hemisphere above the surface. Mathematically

$$\rho(\varphi, \theta) = \frac{\int_0^{2\pi} L'(\varphi', \theta') \cos \varphi' d\omega'}{L_{\varphi, \theta} \cos \varphi(\Delta\omega)} \qquad (1)$$

in which $L_{\varphi, \theta}$ is the incident radiance in the solid angle $\Delta\omega$ about the direction φ, θ: φ is the angle from the normal to the surface and θ is the azimuth from some fixed point on the specimen. $L'(\varphi', \theta')$ is the functional description of the reflected radiance in the direction $\varphi'\theta'$.

*The work described in this paper was done under NASA Contract No. R–09–022–032.
[1] Present address: Dunn Assoc. Inc., 910 Laredo Road, Silver Spring, Md. 20901

Specular reflectance is the fraction of the flux incident in a small solid angle $\Delta\omega$ centered about the direction φ, θ that is reflected into a small solid angle ω' centered about the direction φ', θ', where $\varphi'=\varphi$ and $\theta'=\theta+\pi$. For mirror surfaces, $\omega'=\Delta\omega$, but for engineering surfaces in general, $\omega'>\Delta\omega$. The size of $\Delta\omega$ and ω' should be specified in each case. Mathematically

$$\rho_{\text{specular}}=\frac{\int_{\omega'} L'(\varphi',\theta')\cos\varphi' d\omega'}{L_{\varphi,\theta}\cos\varphi\Delta\omega}. \tag{2}$$

For diffusely reflecting specimens, the defined specular reflectance includes the flux that is diffusely reflected in the specular direction.

Nonspecular reflectance is the directional hemispherical reflectance (eq (1)) minus the specular reflectance (eq (2)).

Directional annular cone reflectance is the fraction of the flux incident in a small solid angle $\Delta\omega$ centered about the direction φ', θ' that is reflected into the annular cone defined by the angles φ_1 and φ_2. Mathematically

$$\rho(\text{d.a.c.})=\frac{\int_{\varphi_1}^{\varphi_2}\int_0^{2\pi} L'(\varphi',\theta')\cos\varphi' \sin\varphi' d\varphi' d\theta'}{L_{\varphi,\theta}\cos\varphi\Delta\omega}.$$

TABLE 1. *Terminology: Flux Terminology*[a]

F_m = The flux reflected by the reference mirror.
F_i = The flux incident on the sample at the first focal point.
F_r = The total flux reflected by the sample (not including interreflections).
F_α = The flux effectively absorbed by the ellipsoidal mirror.
F_w = The flux absorbed by the wire divided by $(\bar{\rho}_\epsilon)_w$. (i.e., F_w is the flux leaving the sample headed in the direction of the wires.)
F_{sp} = The flux that is initially shaded from the detector by the sample divided by $\bar{\rho}_\epsilon$.
F_{sr} = The flux that reaches the detector after multiple reflections with the sample divided by $\bar{\rho}_\epsilon$.
F_h = The flux lost out the entrance hole.
F_s = The total flux crossing the first focal plane (excluding detector ellipsoid interchanges) divided by $(\bar{\rho}_\epsilon)_s$.
F_{s1} = The total flux crossing the first focal plane when shield A_{sh} is used divided by $(\bar{\rho}_\epsilon)_{s1}$.
F_{s2} = The total flux crossing the first focal plane when shield A_{s2} is used divided by $(\bar{\rho}_\epsilon)_{s2}$.
F_d = The total flux crossing the first focal plane when shield A_d is used divided by $(\bar{\rho}_\epsilon)_d$.

[a] All fluxes are defined on the basis of the flux leaving the sample. The subscript D added to the subscript of any of the above fluxes implies the flux actually viewed by the detector when the defined flux is measured by the detector.

Reflectance Terminology

ρ'_ϵ = Effective reflectance of a point on the ellipsoidal mirror.
$\bar{\rho}_\epsilon$ = Effective reflectance of the central area of the ellipsoidal mirror.
$(\bar{\rho}_\epsilon)_s$ = Effective reflectance of the ellipsoidal mirror to the flux F_s.
$(\bar{\rho}_\epsilon)_{s1}$ = Effective reflectance of the ellipsoidal mirror to the flux F_{s1}.
$(\bar{\rho}_\epsilon)_{s2}$ = Effective reflectance of the ellipsoidal mirror to the flux F_{s2}.
$(\bar{\rho}_\epsilon)_d$ = Effective reflectance of the ellipsoidal mirror to the flux F_d.
ρ_{hs} = The hemispherical reflectance of the sample.
ρ_{hm} = The hemispherical reflectance of the reference mirror.
ρ_m = The reflectance of the specular reference standard.
ρ_s = The normal hemispherical reflectance, of a specimen and is approximately equal to $\rho(7°, \theta)$.
$(\bar{\rho}_e)_w$ = The effective reflectance of the ellipsoidal mirror to the flux F_w.
$\rho_{\epsilon d}$ = Effective reflectance of the ellipsoidal mirror to diffuse flux from the second focal point.

Area Terminology

A_h = Area of the entrance hole.
A_ϵ = Area of the opening of the ellipsoidal mirror in the first focal plane minus the area of the shield A_d.
A'_{sh} = Area of the shield A_{sh} in the first focal plane.
A'_s = Area of the sample in the first focal plane.
A'_{s1} = First focal plane area of the image of the sphere entrance port at the second focal point.
A_d = Area of the shield used to block the specular component.
A_{s2} = Represents the shield used to establish the flux distribution for mirror loss corrections.
A_{sh} = Projection of A'_{sh} from the second focal point onto the ellipsoidal mirror.
A_s = Projection of A'_s from the second focal point onto the ellipsoidal mirror.
A_{s1} = Projection of A'_{s1} from the second focal point onto the ellipsoidal mirror.

Angle Terminology

φ = Angle of incidence, measured from the normal to the surface.
θ = Azimuth of incidence, measured from a fixed point on the specimen.
ω = Solid angle of incidence.
φ' = Angle of reflection, measured from the normal to a surface.

Φ' = Azimuth of reflection, measured from a fixed point on the specimen.
ω' = Solid angle of reflection.

Radiance Terminology

L = Radiance of incident flux, watts per steradian per square centimeter (projected normal to the direction of incidence).
$L\varphi, \theta$ = unidirectional radiance.
L' = Reflected radiance.
$L'(\varphi', \theta')$ = Functional description of the reflected radiance in the direction φ', θ'.

Miscellaneous Terminology

η = Efficiency of the averaging sphere (i.e., the ratio of the flux viewed by the detector to that entering the sphere).
η' = The ratio of flux leaving the entrance port of the sphere to that incident on the entrance port.
$f_{s-\epsilon}$ = Diffuse configuration factor from the sphere entrance port to the ellipsoidal mirror (corrected for shading effects of the sample and sample support and for the effect of the entrance hole).

3. Methods of Measuring Reflectance

A reflectometer was desired that would measure absolute reflectance (fraction of incident flux reflected) under conditions approximating normal irradiation and hemispherical viewing, with an accuracy of at least 1 percent, of specimens at temperatures in the range 100 to 800 °K, and over the wavelength range of 1 to 15 μ.

A number of different methods have been used to measure reflectance. Specular reflectance of mirrors [1][2] is of minor interest here, and will not be discussed further. Three different types of reflectometers have been used to measure directional hemispherical reflectance: (1) integrating sphere, (2) hemispherical source, and (3) integrating hemisphere instruments.

(a) *Integrating sphere reflectometers* [2, 3, 4] are widely used at wavelengths below about 2.5 μ, but are generally not suitable for use at longer wavelengths, and will not be discussed further.

(b) *Hemispherical source instruments* measure the reflectance factor[3] under conditions of diffuse irradiation and directional viewing, which is equivalent to directional-hemispherical reflectance. The principal instrument of this type for use in the infrared is the Hohlraum reflectometer [5], in which a cooled specimen is inserted into a heated blackbody cavity, where it is irradiated diffusely. The specimen and a spot on the cavity wall are viewed alternately through an opening in the cavity, and the ratio of the two fluxes is reported as the reflectance. The method is useful in the 1 to 25 μ range. Major errors, that are difficult to eliminate or correct for, arise as a result of heating the specimen and thermal gradients in the cavity walls.

(c) *Integrating hemisphere reflectometers* [6] make use of a hemisphere to focus the flux reflected by a specimen, located at one conjugate focus of the hemisphere, onto a detector located at a second conjugate focus. Major errors, which are difficult to correct for, arise due to spherical aberrations [7], and to variations in areal and angular sensitivity of the detector [8]. Several modifications [9, 10, 11] have been made to the basic Coblentz instrument.

None of the above instruments meets all of the requirements stated at the beginning of this section. Integrating sphere instruments in general are not useful beyond about 2.5 μ. Hemispherical source instruments have no provision for chopping of incident flux, and hence are not suitable for measuring reflectance of hot specimens, and integrating hemisphere instruments have errors because the mirror does not satisfactorily focus the reflected flux and available detectors do not satisfactorily measure the reflected flux. Other disadvantages which limit the usefulness of available reflectometers include (1) errors due to flux losses such as those out entrance and exit ports which are difficult to correct for accurately, (2) lack of versatility; several are restricted by design to measurements under a single set of conditions; and (3) several of them can only be used to measure relative reflectance, and hence require a reference standard calibrated in absolute reflectance, which is not available, in order to give absolute reflectance.

It was decided to build a new reflectometer that would meet all of the requirements previously outlined. The Coblentz hemisphere reflectometer was modified by replacing the hemispherical mirror by an ellipsoidal mirror which permitted the specimen and detector to be separated by about 17 in., and thus permitted heating and cooling of the specimen without affecting the detector. Use of the ellipsoidal mirror, with specimen and detector at true foci, also greatly reduced errors due to spherical aberrations.

4. Design of the Ellipsoidal Mirror Reflectometer [4]

The ellipsoidal mirror reflectometer (EMR) was initially designed in 1959, and construction was completed in 1960 [12]. However, because of serious detector problems [13] and general secondary priority of the work, progress was slow, and the desired results were not achieved until late in 1964.

[2] Figures in brackets indicate the literature references at the end of this paper.
[3] The ratio of the flux reflected directionally by a diffusely illuminated sample to that reflected by the diffuse complete reflector under the same conditions of irradiation and viewing.

[4] Certain commerical instruments and equipment are identified in this paper in order to adequately specify the experimental procedure involved. In no case does such identification imply recommendation or endorsement by the National Bureau of Standards, nor does it imply that the instrument or equipment identified is necessarily the best available for the purpose.

(a) *Basic design.* The basic design of the instrument is shown in figure 1. An ellipsoidal mirror,[5] $12\frac{1}{4}$ in. in diameter and $3\frac{5}{8}$ in. high, is the principal feature of the design. Its focal points are located about $3\frac{5}{8}$ and $20\frac{3}{8}$ in. from the apex, and it has a linear magnification factor of about 5.7.

The flux from a Globar source is chopped at 11.3 c/s and focused on the entrance slit of a Perkin-Elmer Model 83 monochromator. The exit beam from the monochromator is refocused, through a small hole in the ellipsoidal mirror, onto the first focal plane of the ellipsoid, which is in the plane of the edge of the mirror, and centered on the first focal point. A 10-junction thermopile is used as the detector, and its output is amplified by a synchronous amplifier. The angle of incidence of the incident beam on the sample at the first focal point is 7°.

In the absolute mode the incident flux is measured with the detector at the first focal point, and the reflected flux is measured with the specimen at the first focal point and the detector at the second focal point. Thus, after correcting for system losses, the absolute directional hemispherical reflectance is measured for $\varphi = 7°$ (i.e., $\rho(7°, \theta)$). In the relative mode the detector remains at the second focal point, and the fluxes reflected by a standard and the specimen are measured.

[5] Purchased from Strong Electric Corporation, City Park Avenue, Toledo, Ohio.

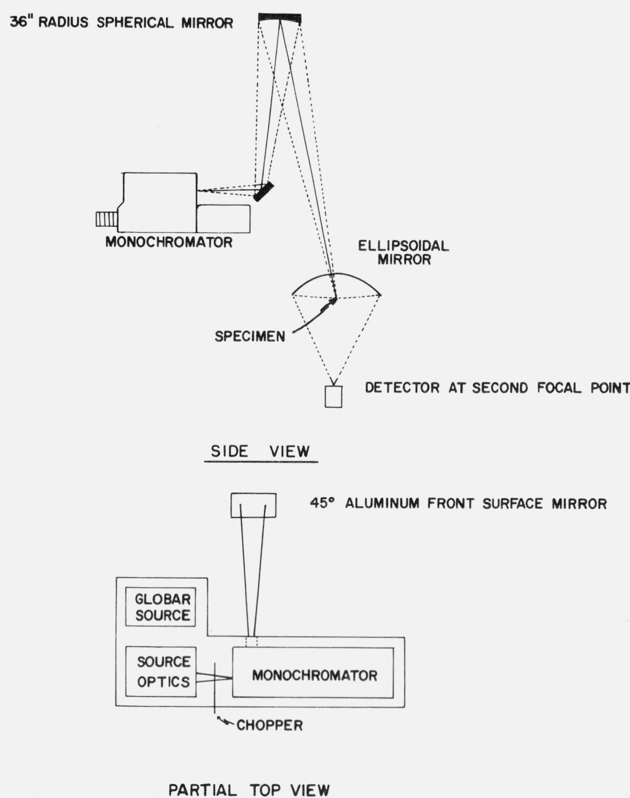

FIGURE 1. *Basic design of the ellipsoidal mirror reflectometer.*

The relative measurement tends to eliminate the errors due to atmospheric absorption and to reduce errors from other sources.

It is more convenient and accurate to use the EMR in the relative mode, first because it is inconvenient and time consuming to move the detector back and forth between the focal points for an absolute measurement, and second because the use of a specular reflectance standard does not introduce a significant error into the measurement, because its reflectance can be measured to about 0.001 [1].

(b) *Advantages of the EMR.* The EMR has the same inherent errors as Coblentz hemisphere systems, with the following exceptions:

(1) Aberrations are reduced [7].

(2) The reflected flux is concentrated in a cone of 24° half angle, instead of a whole hemisphere; hence detector angular sensitivity problems are greatly reduced.

(3) The detector and sample are separated by 17 in., hence the specimen can be heated or cooled without affecting the detector.

(4) The unique optical system permits accurate calibration of mirror and hole losses for practically all engineering surfaces (except diffraction gratings and extremely good retroreflectors).

The optics of the ellipsoidal mirror allow accurate description of the distribution of the reflected flux, because the areal distribution of the reflected energy crossing the first focal plane is related precisely to the geometric distribution of the reflected flux for small areas of irradiation at the first focal point. That is, every direction φ, θ in the hemisphere above the surface is represented by a point P in the first focal plane, and every solid angle centered in the direction φ, θ is represented by an area about P. Thus, it is possible to select the flux that the detector views, by blocking out the unwanted flux with a shield in the first focal plane. Hence, a specular component which has a solid angle determined by the area of the opening in a shield placed in the first focal plane, can be measured. Similarly, the bidirectional reflectance for 7° incidence can be measured by varying the position of a small hole in the shield. The directional annular cone reflectance can be measured by use of a set of circular disks centered on the first focal point. Further, the ability to measure the geometric distribution of the reflected flux enables precise corrections to be made for the system losses, as will be described later.

(c) *Detector problems.* Because of the large magnification factor of the ellipsoidal mirror, about 5.7 linear, a large-area detector is required to view the entire image of the irradiated area. The irradiated area of the specimen is about 2×2 mm in size, and is enlarged to more than 1×1 cm at the detector. When the instrument is used in the absolute mode it must measure equally well the flux in a 2×2 mm image incident in a cone of 4° half angle centered about a direction 7° from the normal, and that in a 1.2×1.2 cm image incident in a cone of 24° half angle centered about the normal.

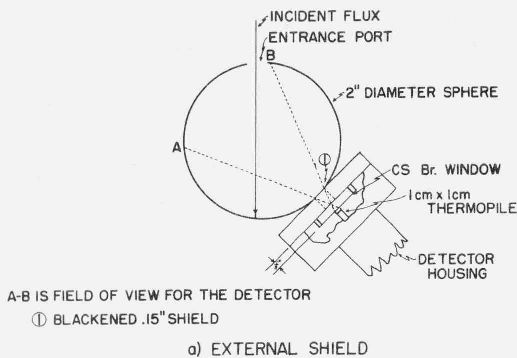

FIGURE 2. *Basic design of averaging sphere.*
The sphere is lined with mμ sulfur.

Preliminary tests, in which a Golay-cell detector and a 10-junction thermopile detector were used, gave reflectances that were in error by 40 to 50 percent. These large errors were later found to be due primarily to the variation in areal sensitivity of the detector [13] and overfilling of the detector sensing area. Detector response to the flux in a 1/16 in. diam beam was found to vary by as much as 50 percent as the beam was scanned across the sensitive area of the detector. There was also some variation of angular sensitivity, particularly at angles from the normal greater than 27°. Detector response to the flux in a 3 by 3 mm beam centered on the sensitive area of the thermopile detector varied only slightly as the angle of incidence was changed from 0° to 27°, but fell off rapidly at angles greater than 27° [14, 15].

(d) *Flux averaging devices.* Several flux averaging devices were investigated [14, 15] and a 2-in. diam sphere lined with mu sulfur, as shown in figure 2, was selected for use with the instrument. Tests using the averaging sphere and the thermopile detector showed that the variation in areal and angular sensitivity of the combination had been reduced to a point where errors from this source could be almost completely eliminated, at wavelengths from the visible out to about 10μ.

5. Analysis of the EMR

In the relative mode the EMR is used to measure the ratio of the flux (F_r) reflected by the sample and the flux (F_m) reflected by the reference standard (e.g., an accurately calibrated mirror); the reflectance $\rho(7°, \theta)$ of the sample is obtained by multiplying this ratio by the reflectance (ρ_m) of the reference mirror, thus:

$$\rho(7°, \theta) = (F_r/F_m)\rho_m. \tag{4}$$

The relation between the flux F_m reflected by the reference mirror and the portion of the flux F_{md} entering the averaging device is simple.[6] The flux F_{md} is the product of the average value of reflectance $\bar{\rho}_e$ of that portion of the ellipsoidal mirror receiving the reflected flux and the reflected flux F_m itself, thus:

$$F_{md} = \bar{\rho}_e F_m. \tag{5}$$

When a diffusing sample is substituted for the reference mirror, however, the relation between the reflected flux F_r and the detected flux may be more complex. There are four major sources of flux loss, and these must all be accounted for precisely: (1) A part, F_α,[7] is absorbed or misdirected by the ellipsoidal mirror, (2) a part F_h is lost out the hole admitting the incident beam, (3) the flux scattered and absorbed by the wire sample supports is $(\rho_\epsilon)_w F_w$,[8] and (4) the flux lost by sample shading is $\bar{\rho}_\epsilon[F_{sp} - F_{sr}]$[9] (see fig. 3).

The flux crossing the first focal plane is $(\bar{\rho}_\epsilon)_s F_s$. Thus, the total flux reflected by the sample is:

$$F_r = F_s + F_w + [F_{sp} - F_{sr}] + F_h. \tag{6}$$

All the fluxes in eq (6) are defined on the basis of the flux leaving the sample, before it is reflected by the ellipsoidal mirror. Since each one of these losses depends on the distribution of flux reflected by the sample, it is necessary to know something about this distribution.

[6] Neglecting until later the interchange of flux between the sample and the averaging device.

[7] Note that the actual mirror loss will be taken into account by considering the reflectance of the ellipsoidal mirror involved in each of the other losses; therefore, F_α does not directly appear in eq (6). Further, the flux terms used in this section are referenced to the flux leaving the sample and not the actual flux loss occurring in each case.

[8] $(\bar{\rho}_\epsilon)_x$ is the average effective reflectance of the ellipsoidal mirror for the given distribution of F_x on the mirror, where x is a variable.

[9] $\bar{\rho}_\epsilon$ is the average effective reflectance of the central part of the ellipsoidal mirror, which varied by less than 0.2 percent. F_{sp} is the flux leaving the sample on the first reflection that is shaded (after reflection from the ellipsoidal mirror) from the sphere entrance. F_{sr} is that part of F_{sp} that eventually reaches the sphere entrance by any path.

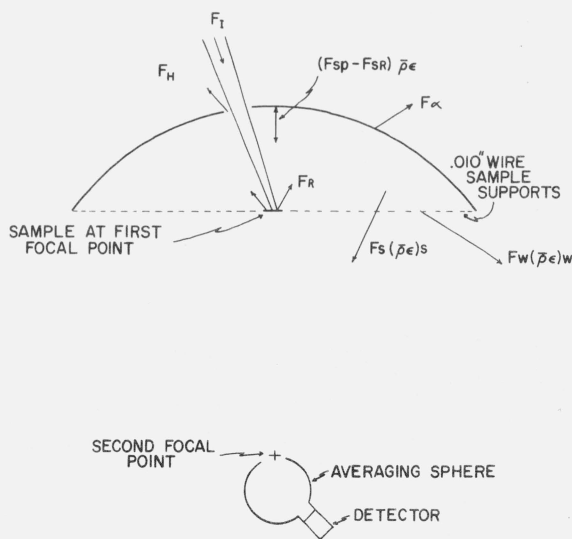

FIGURE 3. *Flux balance of a sample in the ellipsoidal mirror reflectometer.*

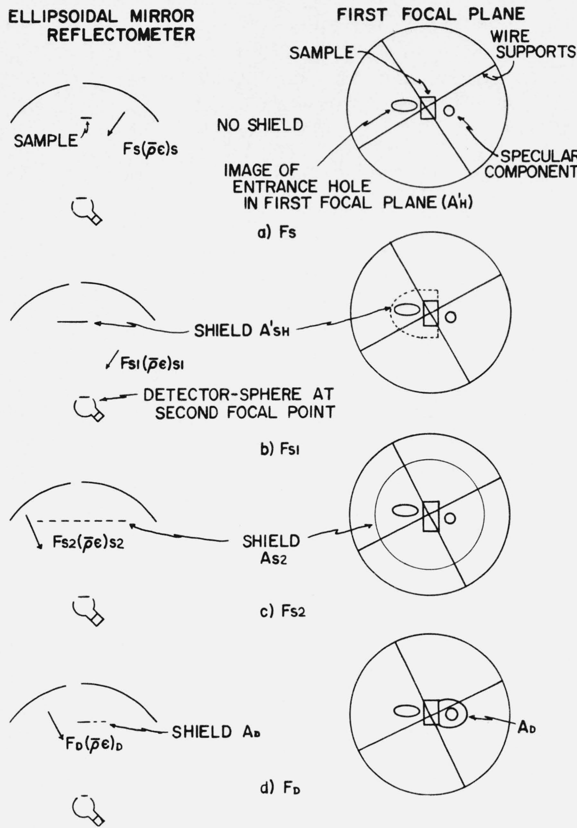

FIGURE 4. *System configuration for definition of the fluxes* F_s, F_{s1}, F_{s2}, *and* F_d.

The flux distribution throughout the system can be evaluated by means of shields placed in the first focal plane, as previously described. Thus, to aid in evaluating the fluxes in eq (6), the following fluxes are defined (see fig. 4):

F_s—the flux crossing the first focal plane, divided by the average effective reflectance of the mirror, for the particular distribution of F_s on the mirror.

F_{s1}—the flux crossing the first focal plane, divided by $(\bar{\rho}_\epsilon)_{s1}$, when shield A_{sh} is in the first focal plane.

F_{s2}—the flux crossing the first focal plane, divided by $(\bar{\rho}_\epsilon)_{s2}$, when shield S2 is in the first focal plane.

F_d—the flux crossing the first focal plane, divided by $(\bar{\rho}_\epsilon)_d$, when shield D is in the first focal plane.

The fluxes defined above can now be used to compute the losses in the system. For brevity, only the equation describing each loss is given. The complete derivation of each loss is given in [15].

Mirror loss, F_α: The ellipsoidal mirror will absorb some of the flux incident upon it. Further, since the mirror is not perfect, it may transmit or scatter some of the incident flux. Thus, it is necessary to know the effective reflectance ρ_ϵ' of the mirror. This is defined as the ratio of the flux that reaches a predefined area at the second focal plane (the entrance port to the averaging sphere) to that incident on the ellipsoidal mirror from a defined area in the first focal plane (the irradiated area of the specimen). The "absorbed" flux ($\alpha = 1 - \rho_\epsilon'$) includes flux lost by absorption, transmission, scattering, and optical aberrations. This ρ_ϵ' was measured for the ellipsoidal mirror, and is reported as a function of position on the mirror in tables 2 and 3. Figure 5 shows the optical paths used in making the measurements and locations of the areas measured. Table 3 indicates that $\rho_{\epsilon n}/\rho_{\epsilon 1}$ does not vary with wavelength, but increases as the measured area moves away from the apex of the mirror. The reflectance of the outer edge of the mirror is about 1.5 percent higher than that of the apex.

TABLE 2. *Absolute reflectance of ellipsoidal mirror (Point 2 in fig. 5)*

	Set #1	Set #2	Set #3	Set #4	Average
1.5 μ	0.951	0.949	0.951	0.948	0.950
2.0 μ	.964	.963	.959	.961	.962
2.5 μ	.965	.969	.967	.963	.966
3.5 μ	.969	.971	.969	.971	.970
4.5 μ	.969	.971	.970	.973	.971
5.5 μ	.970	.971	.973	.970	.971
6.5 μ	.971	.973	.973	.974	.972
7.0 μ	.972	.972	.974	.973	.972

TABLE 3. *Relative reflectance of the ellipsoidal mirror as a function of position and wavelength* [a]

Wavelengths →	1.5 μ	2.0 μ	2.5 μ	3.5 μ	4.5 μ	5.5 μ	6.5 μ	7.0 μ
Areas ↓								
1	1.000	1.000	1.000	1.000	1.000	1.000	1.000	1.000
2	1.001	1.001	1.000	1.000	1.000	1.000	1.001	1.000
3	1.002	1.002	1.001	1.000	1.001	1.001	1.001	1.002
4	1.013	1.010	1.012	1.016	1.016	1.015	1.015	1.013
5	1.000	1.001	1.002	1.001	1.000	1.001	1.000	1.000
6	1.002	1.002	1.003	1.001	1.002	1.002	1.002	1.001
7	1.015	1.013	1.015	1.015	1.014	1.014	1.015	1.013
8	1.001	1.001	1.001	1.000	1.002	1.001	1.001	1.001
9	1.002	1.002	1.003	1.002	1.003	1.002	1.003	1.002
10	1.014	1.015	1.014	1.016	1.015	1.015	1.015	1.014
11	1.001	1.002	1.001	1.000	1.000	1.001	1.001	1.002
12	1.002	1.002	1.001	1.002	1.001	1.002	1.002	1.002
13	1.013	1.014	1.014	1.016	1.014	1.014	1.015	1.014

Average values for areas equally distant from the apex of the ellipsoid

	1.5 μ	2.0 μ	2.5 μ	3.5 μ	4.5 μ	5.5 μ	6.5 μ	7.0 μ
Set A [b]	1.001	1.001	1.001	1.000	1.001	1.001	1.001	1.001
Set B [b]	1.002	1.002	1.002	1.001	1.002	1.002	1.002	1.002
Set C [b]	1.014	1.013	1.014	1.016	1.015	1.015	1.015	1.014

[a] Values are all referred to position No. 1, see figure 3.

[b] Set A is composed of areas 2, 5, 8, and 11; set B is composed of areas 3, 6, 9, and 12; and set C is composed of areas 4, 7, 10, and 13.

If the reflectance of the mirror were uniform, ρ_ϵ would cancel out in the computation of absolute reflectance from relative measurements. Tables 2 and 3 indicate that the flux reflected by a diffusing sample as measured with the EMR should be corrected for the reflectance of the mirror on the basis of its geometric distribution. The defined flux F_{s2} was used to compute the effective reflectance of the mirror for each sample measured. This leads to the following equations for the various effective reflectances of the ellipsoidal mirror.

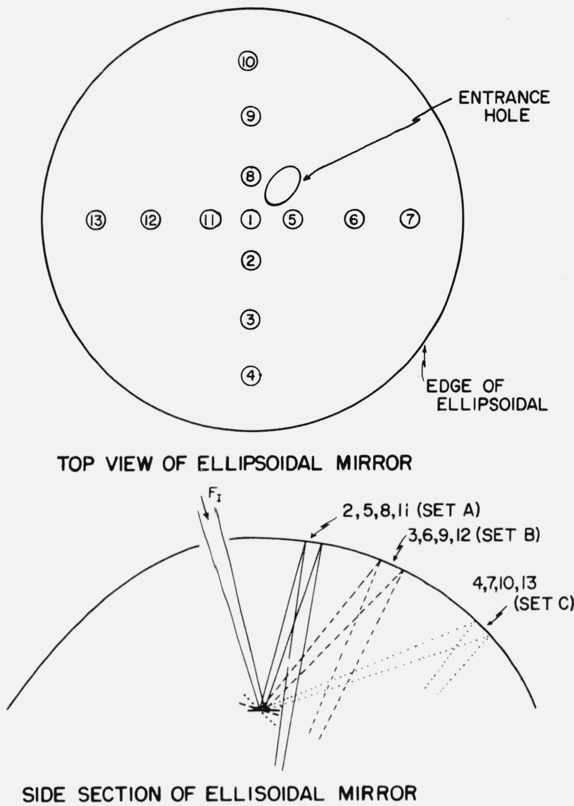

FIGURE 5. *Areas used in measurement of mirror reflectance.*

$$(\bar{\rho}_\epsilon)_s = \bar{\rho}_\epsilon \left[1 + \frac{F_{s2}}{F_s}(0.015)\right] \tag{7}$$

$$(\bar{\rho}_\epsilon)_{s1} = \bar{\rho}_\epsilon \left[1 + \frac{F_{s2}}{F_{s1}}(0.015)\right] \tag{8}$$

$$(\bar{\rho}_\epsilon)_d = \bar{\rho}_\epsilon \left[1 + \frac{F_{s2}}{F_d}(0.015)\right] \tag{9}$$

$$(\bar{\rho}_\epsilon)_{s2} = 1.015\bar{\rho}_\epsilon. \tag{10}$$

Hole loss, F_h: Some of the reflected flux will escape through the hole in the mirror which admits the incident beam. This loss is determined by the amount of flux reflected by the sample in the direction of the hole. Previous investigators have not established the magnitude of this loss, which does not necessarily lie between the condition of no loss for a specular reflector and a loss based on the diffuse configuration factor from the sample to the hole. The flux density around the entrance hole can be computed from fluxes F_s and F_{s1}, as shown in figure 4, and the geometric relationships involved.

$$F_{sh} = F_s - F_{s1} \tag{11}$$

where F_{sh} is the flux incident on the area A_{sh}, the area on the ellipsoidal mirror of the projection of A'_{sh} (in the first focal plane) from the second focal point. Thus, the average flux density around the hole is $F_{sh}/(A_{sh} - A_h)$. It is logical to assume that the flux density over the area of the hole, A_h, is the same as that over the area A_{sh} surrounding it. Thus, the hole loss is

$$F_h = \frac{A_h F_{sh}}{A_{sh} - A_h} \tag{12}$$

or, in terms of the measured fluxes,

$$F_h = \frac{A_h(F_s - F_{s1})}{A_{sh} - A_h}. \tag{13}$$

The assumption of uniform radiance over the small solid angle subtended by A_{sh} is more reasonable and accurate than the assumption of uniform radiance over a hemisphere made by previous investigators.

Wire loss, (F_w): A fraction $F_w(\bar{\rho}_\epsilon)_w$ of the flux reflected by the sample and focused toward the detector will be absorbed or scattered out of the optical path by the wire sample supports. It should be noted that the wires are oriented out of the path of the specularly reflected beam. Hence, if a shield blocks the flux in the area surrounding the direction of specular reflection, the remainder would be the nonspecularly reflected flux. If this flux is assumed to be uniformly distributed over the area (A_ϵ) of the first focal plane of the ellipsoid, then

$$(\bar{\rho}_\epsilon)_w F_w = F_d \frac{A_w}{A_\epsilon} (\bar{\rho}_\epsilon)_d \tag{14}$$

$$\text{where } A_\epsilon = \pi/4 D_\epsilon^2 - A_d. \tag{15}$$

(D_ϵ is the diameter of the ellipsoidal mirror, and A_d is the area of shield D.)

Equation (14) reduces to

$$F_w = F_d(A_w/A_\epsilon) \tag{16}$$

since $(\bar{\rho}_\epsilon)_w \equiv (\bar{\rho}_\epsilon)_d$ when F_d is evenly distributed over A_ϵ.

Since F_w is a secondary correction, it is apparent that the assumption, that the average nonspecular flux density over the first focal plane is intercepted by the wire supports, is sufficiently accurate, especially since the wire supports comprise 2 diam of the first focal plane.

Sample shielding loss, ($F_{sp} - F_{sr}$): Flux leaving the sample normal to its surface will be reflected back to the sample, and hence be blocked from the detector. However, any of the reflected flux incident on the specimen in the area A'_{s1} (the image in the first focal plane formed by the ellipsoidal mirror of the sphere entrance port in the second focal plane) may be multiply reflected by the sample and mirror and focused on the detector. To correct for the sample shielding loss, the three fluxes F_d, F_s, and F_{s1} will be required. The flux involved in this loss is that which

strikes the ellipsoidal mirror on the projected area of the sample, A_s (projected from the second focal point). From figure 4, it is seen that A_s is partially surrounded by the shield A_{sh}, and will have approximately the same flux density as that on A_{sh}. Hence, the total flux initially shaded is

$$F_{sp} = \frac{A_s F_{sh}}{A_{sh} - A_h}. \tag{17}$$

However, a portion A_{s1}/A_s (A_{s1} is the area A'_{s1} projected on the ellipsoid) of the flux F_{sp} is reflected from area A'_{s1} and could reach the detector. Reference 15 shows that the fraction F_{sr} that eventually reaches the detector is

$$F_{sr} = \left[\frac{F_{sh}(A_{s1})}{A_{sh} - A_h}\right] \left[\frac{F_d}{F_s} \rho_s \bar{\rho}_\epsilon \left\{\frac{A_\epsilon - A_w}{A_\epsilon}\right\}\right] \frac{1}{1 - \rho_s \bar{\rho}_\epsilon \left[\frac{F_s - F_d}{F_s}\right]}. \tag{18}$$

The flux multiply reflected by the sample or reference and ellipsoidal mirror that eventually reaches the detector is defined by eq (18), in terms of the four measured fluxes and the area relationships involved.

One further problem arises because the detector is not black; that is, the sphere entrance port back-reflects flux into the optical path, some of which eventually gets back into the sphere and increases the flux sensed by the detector. For the F_s measurement, flux $(\bar{\rho}_\epsilon)_s F_s$ enters the sphere port initially. However, some fraction η' of this flux is reflected back out the sphere entrance port. This flux is reflected nearly diffusely, so that a fraction $f_{s-\epsilon}\eta' F_s(\bar{\rho}_e)_s$ is intercepted by the mirror and focused on the sample in the first focal plane ($f_{s-\epsilon}$ is the standard diffuse configuration factor as defined in reference 16). The sample then reflects the flux back to the mirror, which focuses it on the sphere entrance. Thus, an amount F'_s is added to the flux $F_s(\bar{\rho}_\epsilon)_s$ that was originally incident on the sphere entrance.

$$F'_s = \rho_{hs}(\bar{\rho}_\epsilon)^2_d \eta' f_{s-\epsilon}[F_s(\bar{\rho}_\epsilon)_s] \tag{19}$$

where $(\bar{\rho}_\epsilon)_d$ is the average effective reflectance of the mirror for flux coming diffusely from the sphere entrance and ρ_{hs} is the hemispherical reflectance of the sample. Further, a fraction F''_s of the flux that reaches the sphere on the second pass will be multiply reflected back to the sphere.

$$F''_s = \rho_{hs}(\bar{\rho}_\epsilon)^2_d \eta' f_{s-\epsilon} F'_s. \tag{20}$$

This process will continue until the total flux in the sphere is

$$F_{ss} = (\bar{\rho}_\epsilon)_s F_s \left[\frac{1}{1 - \rho_{hs}(\bar{\rho}_\epsilon)^2_d \eta' f_{s-\epsilon}}\right]. \tag{21}$$

The flux viewed by the detector, F_{sd}, will be

$$F_{sd} = \eta F_{ss} \tag{22}$$

where η is the sphere efficiency.

Similarly, the detector views the other measured fluxes as

$$F_{s1d} = \eta F_{s1}(\bar{\rho}_\epsilon)_{s1} \left[\frac{1}{1 - \rho_{hs}(\bar{\rho}_\epsilon)^2_d \eta'(f_{s-\epsilon})_{s1}}\right] \tag{23}$$

$$F_{s2d} = \eta F_{s2}(\bar{\rho}_\epsilon)_{s2} \left[\frac{1}{1 - \left(\frac{F_s - F_{s2}}{F_s}\right) \rho_{hs}(\bar{\rho}_\epsilon)^2_d \eta'(f_{s-\epsilon})_{s2}}\right] \tag{24}$$

$$F_{dd} = \eta F_d(\bar{\rho}_\epsilon)_d \left[\frac{1}{1 - \rho_{hs}(\bar{\rho}_\epsilon)^2_d \eta'(f_{s-\epsilon})_d}\right]. \tag{25}$$

The total flux reflected by the sample, F_r, is thus

$$F_r = \frac{F_{sd}[1 - \rho_{hs}(\bar{\rho}_\epsilon)^2_d \eta'(f_{s-\epsilon})_s]}{\eta(\bar{\rho}_\epsilon)\left\{1 + \frac{F_{s2d}}{F_{sd}}(0.015)\right\}} \left[1 + \frac{A_h + A_s}{A_{sh} - A_h} - \frac{A_{s1}}{A_{sh} - A_h}\right.$$
$$\left. \times \left\{\frac{F_{dd}}{F_{sd}} \rho_s(\bar{\rho}_\epsilon)^2_d \left(\frac{A_\epsilon - A_w}{A_\epsilon}\right) \left(\frac{1}{1 - \rho_s \bar{\rho}_\epsilon \frac{F_{sd} - F_{dd}}{F_{sd}}}\right)\right\}\right]$$
$$+ \frac{F_{s1d}[1 - \rho_{hs}(\bar{\rho}_\epsilon)^2_d \eta'(f_{s-\epsilon})_{s1}]}{\eta \bar{\rho} \left\{1 + \frac{F_{s2d}}{F_{s1d}}(0.015)\right\}} \left[-\frac{A_h + A_s}{A_{sh} - A_h} + \frac{A_{s1}}{A_{sh} - A_h}\right.$$
$$\left. \times \left\{\frac{F_{dd}}{F_{sd}} \rho_s \bar{\rho}^2_\epsilon \left(\frac{A_\epsilon - A_w}{A_\epsilon}\right) \frac{1}{1 - \rho_s \bar{\rho}_\epsilon \frac{F_{sd} - F_{dd}}{F_{sd}}}\right\}\right]$$
$$+ \frac{F_{dd}[1 - \rho_{hs}(\bar{\rho}_\epsilon)^2_d \eta'(f_{s-\epsilon})_d] A_w}{\eta \bar{\rho}_\epsilon \left\{1 + \frac{F_{s2d}}{F_{dd}}(0.015)\right\} A_\epsilon}. \tag{26}$$

If we now account for the interchange of flux between the reference mirror and the averaging device, the incident flux is computed as

$$F_1 = \frac{F_{1d}[1 - \rho_{hm}(\bar{\rho}_\epsilon)^2_d \eta'(f_{s-\epsilon})_1]}{\rho_m \bar{\rho}_\epsilon \eta}. \tag{27}$$

The reflectance of the sample, $\rho(7°, \theta)$, is equal to the reflected flux, F_r, eq (26), divided by the incident flux, eq (27). The simplifying assumption is made that the terms $(1-\rho_{hs}\bar{\rho}_\epsilon^2\eta' f_{s-\epsilon})$ for F_{1d}, F_{sd}, F_{s1d}, and F_{sdd} are equal, and that η and η' are respectively identical in eqs (26) and (27). Then

$$\rho(7°, \theta)=\frac{\rho_m}{F_{1d}}\left[\left\{\frac{F_{sd}}{\left\{1+\frac{F_{s2d}}{F_{sd}}(0.015)\right\}}\left(1+\frac{A_h+A_s}{A_{sh}-A_h}\right.\right.\right.$$

$$\left.\left.-\frac{A_{s1}}{A_{sh}+A_h}\times\left[\frac{F_{dd}}{F_{sd}}\rho_s(\bar{\rho}_\epsilon)_d^2\left(\frac{A_\epsilon-A_w}{A_\epsilon}\right)\frac{1}{1-\rho_s\bar{\rho}_\epsilon\frac{F_{sd}-F_{dd}}{F_{sd}}}\right]\right)\right\}$$

$$+\frac{F_{dd}}{1+\frac{F_{s2d}}{F_{dd}}(0.015)}\left[\frac{A_w}{A_\epsilon}\right]+\frac{F_{s1d}}{\left\{1+\frac{F_{s2d}}{F_{sd}}(0.015\right\}}\left\{-\frac{A_h+A_s}{A_{sh}-A_h}\right.$$

$$\left.\left.+\frac{A_{s1}}{A_{sh}-A_h}\times\left[\frac{F_{dd}}{F_{sd}}\rho_s\bar{\rho}_\epsilon\frac{A_\epsilon-A_w}{A_\epsilon}\frac{1}{1-\rho_s\bar{\rho}_\epsilon\frac{F_{sd}-F_{dd}}{F_{sd}}}\right]\right\}\right] \tag{28}$$

in which the only remaining unknown is ρ_s, which is identical to $\rho(7°, \theta)$. A very good approximation is

$$\rho_s=F_{sd}/F_{1d}. \tag{29}$$

An error of up to 50 percent in ρ_s, as evaluated by eq (29), would cause only a very small error in $\rho(7°, \theta)$, since ρ_s occurs only in secondary flux terms. If justified, an iteration process can be used to obtain successively better values of ρ_s.

The derivation of eq (28) is, for the most part, applicable to any ellipsoidal mirror. A few of the simplifying assumptions are based on measurement with the particular mirror used in this work.

There are two sources of known errors that are not compensated for in eq (28): they are the edge loss, and detector-sample interchange.

Edge loss. If the sample is not accurately positioned in the first focal plane, some of the reflected flux will miss the ellipsoidal mirror and be lost. The amount depends upon the geometric distribution of reflected flux. For a perfect diffuser, the fraction of the total flux lost in this way is (reference 15)

$$\frac{F_r-F_e}{F_r}=\frac{h^2}{h^2+r_\epsilon^2} \tag{30}$$

where F_r is the total flux reflected by the sample and F_e is the flux hitting the mirror, h is the distance between the sample and the first focal plane, and r_ϵ is the diameter of the ellipsoidal mirror. The magnitude of this loss is shown in figure 6.

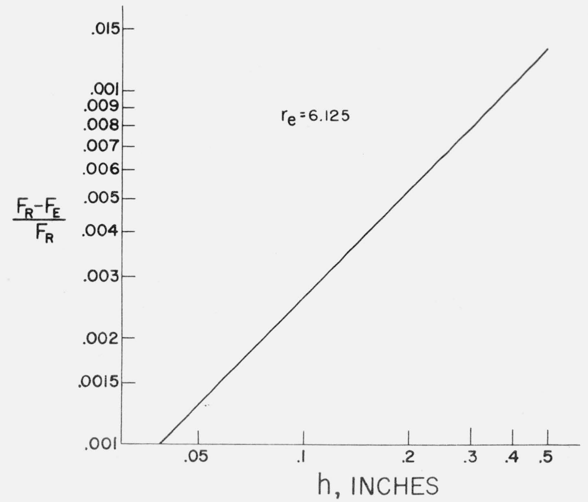

FIGURE 6. *Edge loss for a perfect diffuser.*

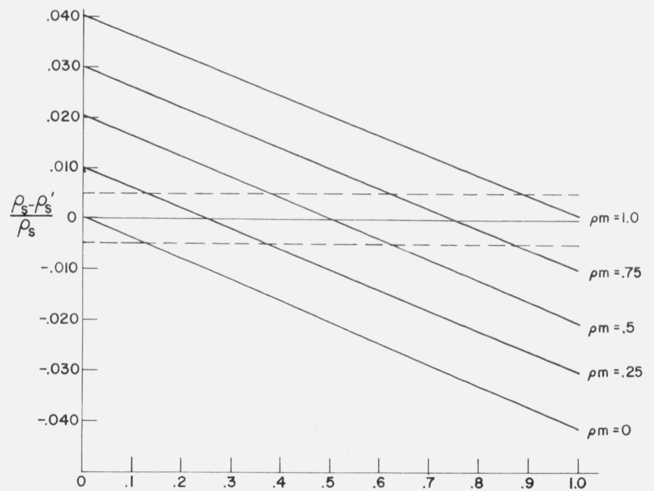

FIGURE 7. *Error due to detector-ellipsoid interchange, for different values of ρ_s and ρ_m.*

Detector-ellipsoid (sample) interchange. In the final steps of the derivation of eq (28), the detector-ellipsoid interchange was ignored. This is legitimate if $\rho(7°, \theta)\cong\rho_m$; however, for $\rho_m \ll \rho(7°, \theta)$ or $\rho_m \gg \rho(7°, \theta)$, a significant error can be introduced from this source. Figure 7 shows the magnitude of this error for different values of $\rho(7°, \theta)$ and ρ_m. The maximum value is 4 percent. The error can be avoided by using a comparison standard having a reflectance ρ_m near that of the sample. If necessary, a calibration can be made for this factor (reference 15).

Summary. The analysis of the EMR presented here is based on the ability to measure four different fluxes. These fluxes, plus a knowledge of the system parameters, permit corrections to be made for system losses, based on reasonable assumptions about the

geometric distribution of flux reflected from surfaces to be measured. The important features of the reflected flux distribution are measured, in order to make accurate corrections. The assumptions on which these corrections are based are believed to be more accurate than those used previously with other reflectometers.

6. Experimental Data

A. *Reference standards.* The use of a calibrated mirror as the reference standard is highly desirable, since suitable mirrors are readily available and can be calibrated by any investigator. The specular reflectometer used in this work to measure the reflectance of the reference mirrors utilized the previously mentioned sulfur-coated diffusing sphere and thermopile detector to measure the incident monochromatic flux and that reflected once each by two sample mirrors. The use of the diffuser reduces the required precision of optical alinement. The ratio of the twice reflected flux to the incident flux is the product of the reflectances of the two mirrors.ˇ If the reflectances are equal, then the ratio is the square of the reflectance. This procedure reduces the error of the measurement, since the expected error is the same whether one or more reflections are involved.

Three sets of four mirrors, each coated with vacuum deposited aluminum, gold, and rhodium, respectively, were used. Six reflectance measurements were made, two each on three different pairs from each set. This did not exhaust the six unique pairs in each set, but allowed intercomparison of all the mirrors to establish that their reflectances are indeed equal. The data are shown in table 4, together with comparable literature values [17, 18, 19, 20].

B. *Optical quality of ellipsoid.* To ascertain that all of the beam of reflected flux was focused onto the entrance port of the averaging sphere at the second focal point, a Polaroid Land camera back was placed at the second focal point so that the plane of the film [10] was at the position of the sphere entrance port. Two different samples were used at the first focal point: (1) an aluminum mirror, and (2) a diffuse porcelain enamel reflectance standard. Figure 8 displays the images formed in the second focal plane for the two different samples and for different exposure times. The black area around each image is the approximate size and shape of the entrance port of the averaging sphere.

The image formed with the aluminum mirror is quite clear and well-defined. The image formed when the mirror was inclined 25° with respect to the first focal plane shows light gray areas surrounding the white image, which indicate that the scatter and aberration of the ellipsoidal mirror increase with distance from the apex. The image formed in the second focal plane when the porcelain enamel (a fairly good diffuser) was placed at the first focal point is enlarged, which indicated that careful location of the image on the sphere entrance port is required if one expects to collect all of the flux represented by these images. The increased image size for the diffuser is indicative of the total scatter and aberrations for this particular ellipsoidal mirror. In all cases, increased time of exposure yielded slightly enlarged images, indicating that a small amount of flux surrounds the visual image. The conclusion drawn from the results displayed in figure 8 is that essentially all of the flux does enter the sphere when care is taken to center the visual image on the entrance.

C. *Directional hemispherical reflectance.* Several samples were chosen for reflectance measurement with the EMR: (1) platinum — 13 percent rhodium alloy, (2) gold mesh, (3) a porcelain enamel, and (4) oxidized Kanthal.[11] Samples 1 and 4 are high-temperature

[10] The film was Polaroid Type 47, a 3000 speed film.
[11] Trade name of a heat-resistant alloy.

TABLE 4. *Measured reflectance of reference mirrors*

λ	Reflectance of aluminum			Reflectance of gold				Reflectance of rhodium	
	Average	Standard deviation	Best literature values [34]	Average	Standard deviation	Literature values [36]	Best literature values [35]	Average	Literature values [37]
1.5	0.9608	0.0012	0.9742	0.9809	0.0014	0.982	0.9906	0.8383	0.882
2.0	.9742	.0017	.9779	.9833	.0010	.983	.9914	.8850	.905
2.5	.9757	.0010	.9794	.9843	.0014	.983	.9922	.9104	.915
3.5	.9828	.0005	.9816	.9870	.0005	.983	.9934	.9339	.932
4.5	.9840	.0011	.9835	.9874	.0008	.983	.9938	.9428	.942
5.5	.9852	.0012	.9850	.9870	.0014	.983	.9938	.9470	.946
6.5	.9852	.0013	.9861	.9878	.0005	.983	.9939	.9474	.950
7.0	.9863	.0017	.9866	.9890	.0017	.984	.9939	9510	.953

$$\text{Average} = \frac{\sum_{1}^{n} \rho}{n}.$$

$$\text{Standard deviation} = \sqrt{\frac{\sum_{1}^{n} (\rho - \bar{\rho})^2}{(n-1)}}.$$

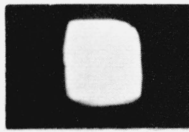

Aluminum Mirror
0° Sample Holder
2-Second Exposure

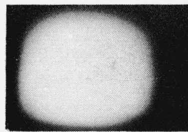

Enamel
0° Sample Holder
2-Second Exposure

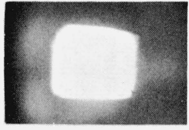

Aluminum Mirror
0° Sample Holder
1-Minute Exposure

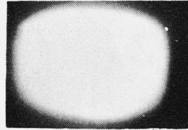

Enamel
0° Sample Holder
15-Second Exposure

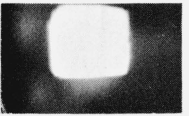

Aluminum Mirror
25° Sample Holder
5-Second Exposure

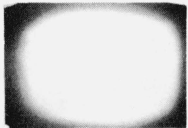

Enamel
0° Sample Holder
45-Second Exposure

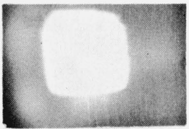

Aluminum Mirror
25° Sample Holder
1.5-Minute Exposure

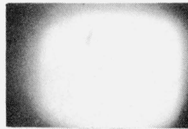

Enamel
0° Sample Holder
2-Minute Exposure

FIGURE 8. *Photographs of images formed in second focal plane of ellipsoidal mirror.*
The black area surrounding each image is the approximate size of the sphere entrance port.

emittance standards provided by the National Bureau of Standards and described by Richmond et al., [21]. Sample 2 was provided by Bernd Linder of the Missiles and Space Division, General Electric Company, Philadelphia, Pa. It is a 0.002-in. diam stainless steel wire screen, 135 mesh, backed by 1.5 mil Mylar, coated with vapor-deposited gold. Sample 3 is a standard of luminous daylight reflectance.

(1) *Platinum-13 percent rhodium.* The average values obtained in six determinations of the reflectance of each of two samples are shown in figure 9. Table 5

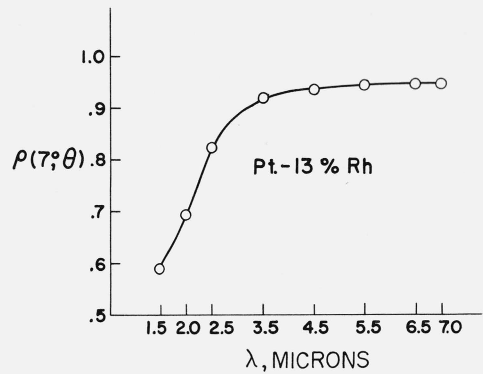

FIGURE 9. *Spectral directional hemispherical reflectance of platinum-13 percent rhodium alloy.*
Each point is the average of six determinations, three each on two specimens.

gives the individual measurements, and values from reference 21. The six values reported in table 5 were obtained by two different operators over a period of one week. Determinations 1a and 2a were made on samples tilted 10° to the first focal plane, in order to eliminate the hole and sample shading corrections. This is possible because, as the data on the specular component in table 5 indicate, the reflected flux is concentrated around the specular direction, and tilting the sample results in no edge loss. The data for the tilted samples are not significantly different from those for samples that were not tilted: hence, the corrections must have been accurate (assuming no change of reflectance for small change in angle of incidence).

(2) *Gold mesh.* The data for the gold mesh samples are presented in figure 10. Each data point is the average of three determinations.

(3) *Porcelain enamel.* The data for the porcelain enamel reflectance standard are presented in figure 11. No attempt was made to correct for the sphere-ellipsoid interchange.

(4) *Oxidized Kanthal.* The data for the oxidized Kanthal are shown in figure 12. The incident flux was attenuated by 50 percent with a sector disk for the reference measurement, but not for the sample measurement. The data were corrected for the sphere-ellipsoid interchange [15].

The data in figures 7, 8, 9, and 10 include a value for the specular component of reflected flux. No effort was made to study the size of the shield that would give the most useful specular component: instead, the A_{sh} shield was used. The specular component was computed as:

$$\%\text{ specular component} = \frac{F_{sd} - F_{dd}}{F_{sd}} \times 100. \quad (31)$$

The experimental specular component for a near perfect diffuser (mu sulfur) is 9 percent. The "true" specular component is that computed by eq (31) minus 9 percent, and is shown in table 6.

208-651 O-66—3

TABLE 5. *Reflectance of platinum—13 percent rhodium alloy* [a]

Wavelength	# 1a	# 1b	# 1c	# 2a	# 2b	# 2c	Average	Standard deviation	Specular component [b]
									%
1.5	0.610	0.597	0.591	0.566	0.574	0.603	0.596	±0.005	69
2.0	.701	.691	.692	.694	.686	.696	.693	.002	82
2.5	.823	.813	.821	.826	.827	.820	.822	.002	83
3.5	.919	.905	.921	.924	.930	.913	.919	.005	86
4.5	.933	.926	.937	.935	.940	.929	.933	.004	87
5.5	.942	.936	.940	.946	.947	.932	.941	.005	88
6.5	.945	.938	.940	.947	.949	.942	.944	.005	90
7.0	.947	.940	.942	.946	.953	.943	.945	.005	92

[a] The specimens were annealed at 1825 °K prior to measurement. Two samples are represented in this table, 1 and 2. Measurements 1a and 2a were made with the sample tilted 10° to the first focal plane.

[b] This is an approximation of the specular component by using $[(F_{sd}-F_{dd})/F_{sd}]\times 100\%$, because it includes the diffuse component of flux in the solid angle about the specular direction, and does not account for obvious system corrections.

NBS Reflectance for Pt 13% Rh reference 38 (various sample temperatures) [c]

λ	800 °K	1100 °K	1300 °K
	%	%	%
1.5 μ	74.8	78.7	77.4
2.0	80.8	81.5	80.3
2.5	83.5	83.2	82.0
3.5	87.4	85.7	84.5
4.5	89.1	87.4	86.5
5.5	90.4	88.9	87.3
6.5	91.4	89.9	88.7
7.0	91.6	90.4	89.2

[c] Data are $1-\epsilon$, where ϵ is normal spectral emittance.

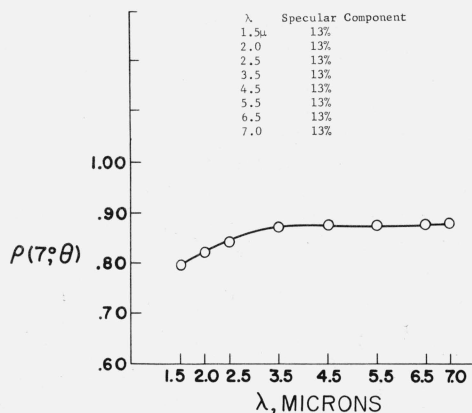

FIGURE 10. *Spectral directional hemispherical reflectance of gold mesh.*

Each point is the average of three determinations.

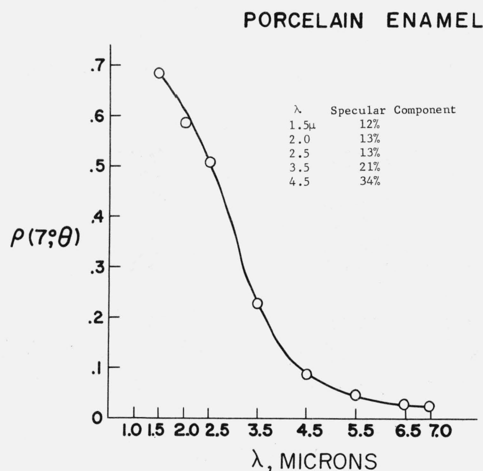

FIGURE 11. *Spectral directional hemispherical reflectance of a porcelain enameled specimen.*

D. *Directional annular cone reflectance.* The directional annular cone reflectance of samples of Crystex brand sulfur, $BaSO_4$, and gold mesh was measured at 2.5 μ and compared to the values computed for the perfect diffuser. The directional annular cone reflectance ρ(d-a-c) is defined as follows

$$\rho(\text{d-a-c})=\frac{\int_0^{2\pi}\int_{\varphi_1}^{\varphi_2} L'(\varphi',\theta')\cos\varphi'\sin\varphi' d\varphi' d\theta'}{L(7^\circ,\theta)\Delta\omega}. \tag{32}$$

In the direct measurements, φ_2 was always $\pi/2$, and the flux reaching the detector was restricted to the annular solid angle between φ_1 and $\pi/2$ by means of a circular disk centered on the sample and placed just below the first focal plane. Five shields were used to obtain five different values of φ_1. In each case, the reading with a shield in place was divided by F_r to obtain the ratio of the directional annular cone reflectance to the directional hemispherical reflectance. By subtracting the values obtained with successively larger shields, it was possible to separate the hemispherical reflectance into five annular cone

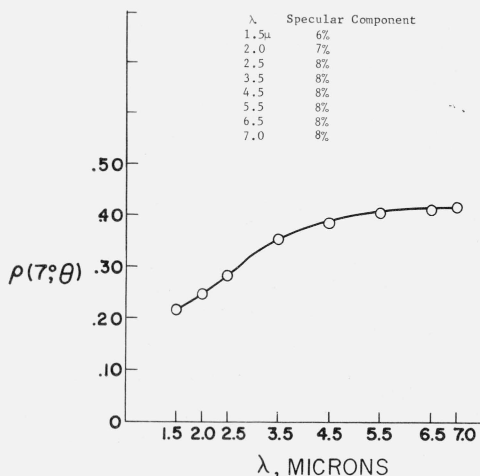

FIGURE 12. *Spectral directional hemispherical reflectance of oxidized Kanthal.*

TABLE 6. *"True" specular components*

λ	Pt-13% Rh	Gold mesh	Porcelain enamel	Oxidized Kanthal
Microns	%	%	%	%
1.5	60.0	4.0	3.0	−3.0
2.0	73.0	4.0	4.0	−2.0
2.5	74.0	4.0	4.0	−1.0
3.5	77.0	4.0	12.0	−1.0
4.5	78.0	4.0	25.0	−1.0
5.5	79.0	4.0	....	−1.0
6.5	81.0	4.0	....	−1.0

reflectances. These are compared to the computed ratio for a perfect diffuser in table 7. It should be noted that the specific measurement technique used will not yield the most accurate data since these data were not corrected for various system losses.

TABLE 7. *Ratio of directional annular cone reflectance at 2.5 μ to the directional hemispherical reflectance for diffusely reflecting samples*

φ_1°	φ_2	Perfect diffuser	Crystex sulfur	$BaSO_4$	Gold mesh
0	14.5	0.06	0.07	0.07	0.08
14.5	34.3	.25	.24	.25	.28
34.3	43.7	.16	.17	.16	.16
43.7	62.8	.31	.32	.31	.29
62.8	79.5	.18	.17	.17	.16
79.5	90.0	.03	.04	.04	.03

It can be seen from the tables that the barium sulfate comes closest to being a perfect diffuser, and that the sulfur is also a very good diffuser. While the gold mesh reflects an appreciable percentage into each of the annular cones, it reflects more than a perfect diffuser at angles less than 34.3°, and less than a perfect diffuser at angles from 43.7° to 79.5°. This can be interpreted to indicate appreciable increase in reflection in specular and near specular directions.

7. Summary and Conclusions

An ellipsoidal mirror reflectometer was designed and built. It consists essentially of (1) a source of monochromatic flux, (2) an ellipsoidal mirror reflector, and (3) a detector. A beam of chopped monochromatic flux from a monochromator equipped with a Globar source is focused through a small hole in the ellipsoidal mirror onto the specimen, which is centered on the first focal point of the ellipsoid. The reflected flux is collected by the ellipsoidal mirror, and focused onto the detector, which is centered on the second focal point. The incident flux is measured (1) (in the absolute mode) by moving the detector to the first focal point, and measuring it directly, or (2) (in the comparison mode) by substituting a mirror of known reflectance for the specimen. It should be emphasized that the reflectometer measures reflectance in absolute units by both techniques.

Serious problems were encountered, that led to errors on the order of 50 percent of the measured reflectance. These large errors were found to be due to the variation in spatial and angular sensitivity of the detector and over-filling of the detector sensitive area. These errors were eliminated by use of a sulfur-coated averaging sphere on the detector.

Because of the unique optical system, each direction from the first focal point of the ellipsoid toward the mirror corresponds to a point in the first focal plane, and each solid angle from the first focal point corresponds to an area in the first focal plane. Hence, it is possible, by the use of shields in the first focal plane, to measure the flux reflected in any desired solid angle about any desired direction. In this way, accurate estimates can be made of all known losses, and corrections applied. This also permits measurement of (1) directional-hemispherical reflectance, (2) specular reflectance, (3) nonspecular reflectance, and (4) directional annular cone reflectance.

An analysis of all known errors leads to the conclusion that the instrument is capable of measuring directional-hemispherical reflectance to an accuracy of at least 0.01 [15].

Data are presented on the directional-hemispherical reflectance at wavelengths from 1.5 to 7.0 μ of annealed platinum-13 percent rhodium alloy, gold mesh, a porcelain enamel, and oxidized Kanthal; in addition, the specular component of reflected flux is separately evaluated for these materials. Data are also presented on the directional annular cone reflectance of the gold mesh, barium sulfate, and Crystex brand sulfur.

The assistance of Warren D. Hayes, Jr., and David P. DeWitt in construction of the equipment and early testing; and of John T. Perone, Jr., in making many of the measurements, is gratefully acknowledged.

8. References

[1] Bennett, H. E. and Koehler, W. F., Precision measurement of absolute specular reflectance with minimized systematic errors. J. Opt. Soc. Am. **50,** 1–6 (1960).

[2] Parmer, J. F., The thermal radiation characteristics of specular walled grooves in the solar space environment, Ph.D. Thesis, Oklahoma State University, May 1965.

[3] Edwards, D. K., Gier, J. T., Nelson, K. E., and Raddick, R. D., Integrating sphere for imperfectly diffuse samples, Appl. Opt. **51,** 1279–1288 (1961).

[4] Jacques, J. A. and Kuppenheim, H. F., Theory of the integrating sphere, J. Opt. Soc. Am. **45,** 460–470 (1955).

[5] Gier, J. T., Dunkle, R. V., and Bevans, J. T., Measurement of absolute spectral reflectivity from 1.0 to 15 microns. J. Opt. Soc. Am. **44,** 558–562 (1954).

[6] Coblentz, W. W., The diffuse reflecting power of various substances, Bull. BS **9,** 283–325 (1913).

[7] Brandenberg, W. M., Focusing properties of hemispherical and ellipsoidal mirror reflectometers, J. Opt. Soc. Am. **54,** 1235–1237 (1964).

[8] Stair, R. and Schneider, W. E., Standards, sources, and detectors in radiation measurements, Symposium on Thermal radiation of solids, ed. Dr. Samuel Katzoff, NASA SP–55. To be published in 1965.

[9] Janssen, J. E. and Torborg, R. H., Measurement of spectral reflectance using an integrating hemisphere. Measurement of Thermal Radiation Properties of Solids, ed. J. C. Richmond. NASA SP–31, 1963, pp. 169–182.

[10] White, J. U., New method for measuring diffuse reflectance in the infrared, J. Opt. Soc. Am. **54,** 1332–1337 (1964).

[11] Kozyrev, B. P. and Vershinin, O. E., Determination of spectral coefficients of diffuse reflection of infrared radiation from blackened surfaces, Optics and Spectroscopy **6,** 345–350 (1959).

[12] Harrison, W. N., Richmond, J. C., Plyler, E. K., Stair, R., and Skromstad, H. K., Standardization of Thermal Emittance Measurements. WADC Technical Report 59–510 Pt. II (Nov. 1960).

[13] Richmond, J. C., DeWitt, D. P., Dunn, S. T., and Hayes, W. D., Jr., Procedures for the Precise Determination of Thermal Radiation Properties, November 1963 to October 1964. Technical Documentary Report ML–TDR–64–257 Pt. II, Materials Laboratory, U.S. Air Force (1965).

[14] Dunn, S. T., Flux averaging devices for the infrared, NBS Tech. Note 279, 1965.

[15] Dunn, S. T., Design and analysis of an ellipsoidal mirror reflectometer, Ph.D. Thesis, Oklahoma State University, 1965.

[16] Wiebelt, J. A., Engineering Radiation Heat Transfer, (Hott, Rinehart and Winston, 1965).

[17] Bennett, H. E., Silver, M., and Ashley, E. J., Infrared reflectance of aluminum evaporated in ultra-high vacuum, J. Opt. Soc. Am. **53,** 1089–1095 (1963).

[18] Bennett, J. M. and Ashley, E. J., Infrared reflectance and emittance of silver and gold evaporated in ultrahigh vacuum, Appl. Opt. **4,** 221–224 (1965).

[19] Hass, G., Optics Section, American Institute of Physics Handbook, pp. 6–19, Coordinating Editor: D. E. Gray, 1957, (McGraw-Hill Book Company, Inc., New York, N.Y.)

[20] Hass, G., Filmed surfaces for reflecting optics, J. Opt. Soc. Am. **45,** 945–952 (1955).

[21] Richmond, J. C., DeWitt, D. P., and Hayes, W. D., Jr., Procedures for precise determination of thermal radiation properties, November 1962 to October 1963, NBS Tech. Note 252, 1964.

(Paper 70C2–221)